Environ Monit Assess (2018) 190: 512
https://doi.org/10.1007/s10661-018-6890-1

Suitability of open-access elevation models for micro-scale watershed planning

Arif Oguz Altunel

Received: 9 February 2018 / Accepted: 2 August 2018 / Published online: 10 August 2018

Abstract Watershed planning is a major issue in Turkey and other parts of the world. Surrounded by seawater on almost three-quarters of its international borders and by sheer mountains along the coastal regions and throughout the country, Turkey experiences a range of climatic changes, which constantly shape its topography. Recently, the occurrences of floods, landslides, and torrents have increased, forcing decision-makers to come up with solutions to manage and rehabilitate the upper watersheds in order to stop or limit the impact of disasters on downstream areas. Possible solutions should reduce flow coefficients, erosion, and sedimentation and increase reservoir capacities. It is expected that torrent volumes will decrease, drainage regimes on slopes will be better organized and adjusted, thawing snow will be better deposited and delayed, evapotranspiration will increase, surface runoffs will be delayed, and water regimes will be better managed, meaning that flood and torrent control will be achieved. For the reasons mentioned above, watershed parameters need to be firmly set. In the scope of this study, the elevation, slope acreage, and reservoir capacity of a small watershed, as extracted from open-access elevation models, were compared to a real-time kinematic (RTK) global positioning system (GPS)-generated point cloud and the resulting elevation model through various geospatial and analytical means. The Shuttle Radar Topography Mission (SRTM) C-band digital elevation model (DEM) (version 3) proved to be a satisfactory method in making residual, correlation, mean, and reservoir capacity comparisons. An L-band Advanced Land Observing Satellite (ALOS) phased-array-type synthetic aperture radar (PALSAR) and an X-band DLR_SRTM ASTER were slightly superior methods in terms of defining a greater number of slope categories than the other models. Finally, DLR_SRTM and SRTMv3 could match a greater number of slope façades than the other models. Seventeen years after its acquisition, SRTM and its derivatives have continued leading the topographic definition of the Earth.

Keywords Watershed parameters · Elevation models · GIS

A. O. Altunel (✉)
The Department of Forest Engineering, Faculty of Forestry, Kastamonu University, 37150 Kastamonu, Turkey
e-mail: aoaltunel@kastamonu.edu.tr

Introduction

Turkey, also called Anatolia or Asia Minor, is situated between Europe and the Arabian Peninsula. It is a diverse country with various geographical features owing to its location. The average elevation is 1132 m above sea level, and 62.5% of its land area has a slope gradient of more than 15%. Twenty-nine percent of the Anatolian land area can be considered as medium to high, whereas an additional 27% of it can be considered as a mountainous terrain. Areas with an elevation of 1000 m or higher correspond to 56% of the Anatolian land. Short-term extreme climatic conditions and precipitation rates are widespread and are on the rise

(Tayanc et al. 2009). When it rains on steep, mountainous, and barren topography, the rain quickly turns into surface runoff (Munir and Iqbal 2016), and the intensified momentum of the surface runoff causes floods and torrents on the lower elevations (Golding et al. 2016). Rapidly accelerating surface runoff exacerbates soil erosion, and productive topsoil is removed and transported to ponds, reservoirs, lakes, and seas (Mei et al. 2016), thus shortening the economic lifespans of these water features (Asmamaw 2015; Turker and Acikgoz 2006). Due to the fact that floods and torrents cause extensive damage to infrastructures and can result in human fatalities (Mahmood et al. 2016), they are ranked second after earthquakes in terms of natural disasters (Bolt et al. 2013). The International Disasters Database reported that Turkey has experienced 1798 deaths due to floods and landslides between 1948 and 2015 (EM-DAT 2009). There are 227 designated torrent/landslide-generating watersheds throughout the country, and flood control measures have been implemented over 41,552 km^2 since 2013. Afforestation, erosion control, terracing, slope, ephemeral creek/stream, range, and unproductive forest rehabilitation works are jointly carried out by the Forest Service and State Hydraulic Works in order to tackle these problems. The fact that the country's topography is rugged and treacherous and that its semiarid climate leads to heavy precipitation resulting in flash floods on extremely erosion-susceptible soils has caused Turkey to devise solutions to mitigate such adverse effects (Ceylan et al. 2007).

Conceptually, watershed management deals with either structural (engineering) or nonstructural (vegetative) practices or both of them to solve these erosion problems. An integrated watershed management approach must evaluate and aggregate the actual physical properties of a watershed as well as the political facts resulting from the demands of people (Turner et al. 2014). Structural practices require careful planning before any field implementation. To this end, digital elevation models (DEMs) provide invaluable feedback to decision-makers. DEMs can be defined as the representation of a topographic surface, a sampled set of spatial coordinates (x, y, z) that are shaped using a suitable interpolation function (Aguilar et al. 2005). A number of parameters, such as aspect, slope, contours, drainage networks and delineation, and surface roughness, can be extracted from DEMs, and numerous surface-related functions, such as hillshades and viewsheds, can be derived (Yang et al. 2011). Thus, watershed scale management strategies could be envisioned and devised from virtual settings that have analytical capabilities (Benda et al. 2016).

Data obtained by means of tachometric surveying (Grussenmeyer et al. 2008), stereo-acquired aerial photography (Nichol et al. 2006), digitization of contour lines from topographical maps (Kweon and Kanade 1994), stereo-acquired satellite imagery (Berthier et al. 2010), interferometry (Rufino et al. 1998), airborne laser scanning (Risbøl et al. 2015), light detection and ranging (Pradhan and Abdulwahid 2017), and unmanned aerial vehicles (Uysal et al. 2015) are widely accepted and used for DEM generation. All DEMs generated using any of the above methods include some degree of error, which is unavoidable most of the time. The accuracy of a DEM is validated by comparing a DEM surface with the relative measurements from the corresponding actual topography. For example, a DEM acquired by digitizing the contour lines of a topographical map can be compared either to an actual field or to a photogrammetric survey. Thus, positive or negative differences can be statistically tested to determine whether the DEM in question is suitable. Topographical conditions (Patel et al. 2016), GRID spacing, and interpolation functions (Goulden et al. 2016) affect the overall accuracy and consistency of DEMs.

Today, the know-how and the technology required to build a near-perfect representation of a topographical surface are widely available and keep improving. However, as the area to be measured increases, the effectiveness and feasibility of the proven methods start diminishing in terms of time and finances. Thus, space-borne technology is once again a promising lead for tackling such issues. In the present study, we look into the efficiencies of open-access elevation models for defining a few watershed parameters in a small watershed.

Five previously released open-access elevation models—the Shuttle Radar Topography Mission (SRTM) C-band DEM (version 3) by NASA, Space-Borne Imaging (SIR) and X-band DEM by the German Aerospace Center (DLR) and Italian Space Agency (ASI), Synthetic Aperture Radar (SAR), ALOS Palsar, phased-array-type L-band SAR DEM, and ASTER GDEM generated through stereosatellite imagery (versions 1 and 2)—were compared to an elevation model formed from a real-time kinematic (RTK) global positioning system (GPS)-generated point cloud.

DEM or digital surface model creation is not limited to the platforms and instruments mentioned above. Currently, other operating systems, such as the French

SPOT-DEM, the Indian CARTOSAT-1-DEM, and the German Tandem-X Mission World-DEM, are also used. However, SRTMs, ALOS, and GDEMs are the only systems that provide near-global surface coverage free of charge, which is why they have been used in this study.

An overwhelming number of studies have been conducted on the precision of the conformity of such elevation models to actual land surface(s) through elevation points or cross-sectional comparisons (Grohmann 2015; Józsa et al. 2014; Anornu and Kortatsi 2012; Mispan et al. 2015). GRID spacing and positioning affect the positions of the elevation points. So, despite being similar on the broader scale, DEMs produced from different sources differ considerably in minute details. Therefore, we independently tested three watershed-defining parameters—elevation, slope, and reservoir capacity—in order to assess which of the open-access DEMs produce a better fit to the actual topographical surface.

Materials and methods

Study area

This study was conducted on a dam reservoir located around 41° 22′ 44″ N and 34° 00′ 17″ E on a 200-ha area in the subprovince Taşköprü within the province of Kastamonu in north-central Turkey (Fig. 1). The elevation ranged between 750 and 990 m above sea level. The State Hydraulic Works was in the process of drafting engineering plans and structures for a proposed irrigation/flood control dam. Therefore, a high-precision elevation model was needed. A freelance surveyor surveyed the dam reservoir and the surrounding areas and generated a point cloud encompassing 27,307 location points with x- and y-coordinates and z values using an RTK/continuously operating reference system (CORS) and a GPS receiver. The Turkish cadastral precision requirement for such receivers dictates that the location errors in all dimensions must be less than or equal to 3 cm (Deniz et al. 2008). Given that the area in question has been used as a grazing meadow for over 20 years and was only covered with grassy vegetation and occasional waist-deep brushes, a high degree of surveying precision was achieved. The data were collected for a month, starting in May 2014. The longevity of the abovementioned labor-intensive surveying and the associated service charge paid for it were the justifying reasons to find rather reasonable and easily attainable alternative means to supply such varying-scale undertakings.

Modeling procedures and data handling

The point cloud was acquired from the State Hydraulic Works. On checking the data in detail, it became apparent that the method of recording the point locations was not based on a preset GRID spacing, but the points were rather irregularly spaced from the top to the bottom as the surveyors traversed through the watershed (Fig. 2). From the frequency of the RTK-GPS-measured location points, it was apparent that the surface model to be created using this point cloud would include many fine details of the topography. Therefore, the datasets acquired from the open-access elevation models were investigated to see whether the measured values could satisfactorily be estimated from them. Another point cloud with large-interval recordings, spanning a larger or a regional area, would be more suitable to test the performances of such models; however, only comparison of the elevation (vertical accuracy) would be achievable. The remaining or additional parameters could not be extracted, because the actual measurements would be too far away from one another to accurately depict the actual surface (Gao 1997). For the reason mentioned above, this study should not be considered as a case study for a specific location. However, it can be considered as a study that evaluates how more detailed results could be generated from open-access elevation models in close quarters.

Although the point locations were not systematically recorded, their distribution and frequent recording showed that they would be sufficient to build a high-precision triangular irregular network (TIN) model of a watershed. TIN is one of the main alternatives to GRID-spaced DEMs in terms of data storage efficiency and structural simplicity (Kang et al. 2015).

Once the elevation model of the watershed was built, the search for alternative data sources was carried out. C-band SRTM (SRTMv3) and ASTER GDEM versions 1 and 2 (GDEMv1 and GDEMv2) datasets were downloaded from the US Geological Survey's Earth Explorer global data portal, the X-band DLR_SRTM (DLR) dataset was downloaded from DLR's EOWEB geoportal, and the L-band ALOS PALSAR (ALOS_P)

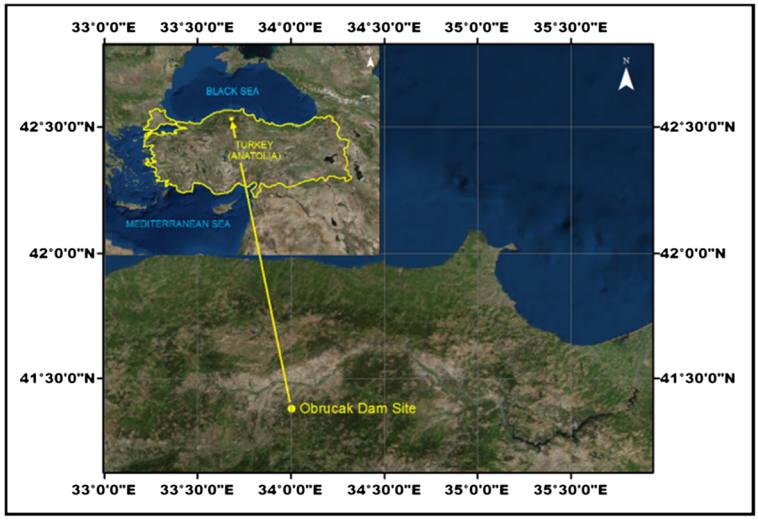

Fig. 1 Location of study area

datasets were downloaded from the Alaska Satellite Facility's Vertex data portal.

The point cloud of the Obrucak Dam Site was generated, specifying the Transverse Mercator map projection with 3° longitudinal spans over the Geodetic Reference System GRS80 ellipsoid, all together named ITRF-96. Turkey used the Gauss-Krüger 3° Transverse Mercator map projection and the European Datum 1950 ED50 up until 1999. Then, a consensus to appropriate a new system was agreed upon, and the International Terrestrial Reference Frame ITRF-96 was adopted. The Turkish General Cadastral Directorate dictates that all cadastral surveys and measurements must be conducted using the new system for improved accuracy (Deniz et al. 2008). Compliance with other projections and datums is achieved through transformations. Therefore, the previously mentioned point cloud was first reprojected to ED50 using some transformation parameters and then to the World Geodetic System "WGS84" datum, in which no projection transformations were performed.

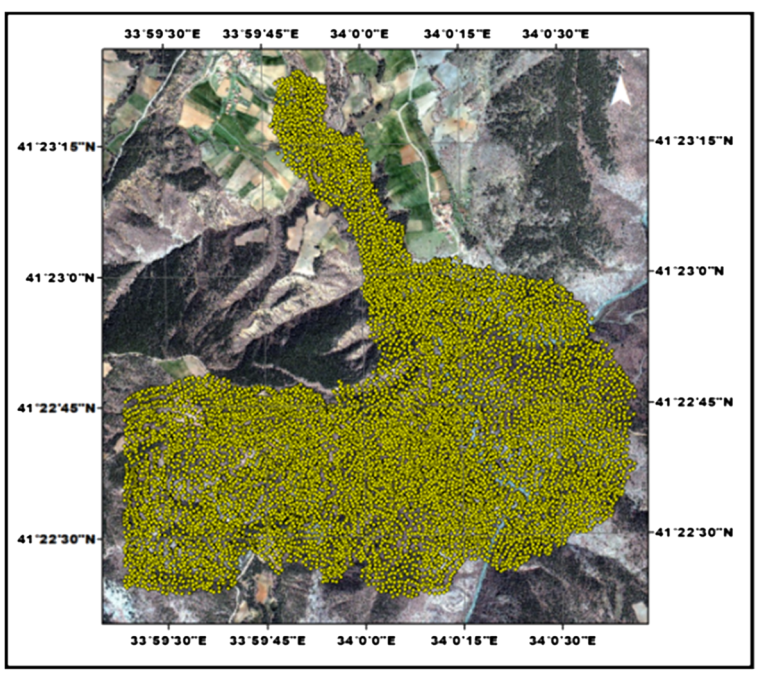

Fig. 2 Point cloud used to model the watershed

Open-access DEMs, by contrast, are stored and disseminated and have geographic (latitude and longitude) projection and WGS84 datum. Thus, they were only reprojected to the "Transverse Mercator" projection, and no datum transformation was performed. ArcGIS 10 was used in all stages of the analysis.

Once all the datasets were defined in equal terms, the proposed watershed parameters, namely elevation, slope (acreage), and reservoir capacity, were first extracted from the model using the point cloud and then compared to the parameters extracted from the other models, using the open-access DEMs. Elevation values for z were obtained from the x- and y-coordinates of the point cloud and compared to the raster DEM-extracted values obtained from the same x- and y-coordinates. Slope (acreage) maps were produced using the raster DEM and compared to those of the open-access datasets. The reservoir capacity calculated using the TIN model based on the point cloud was compared to TIN models built from the open-access datasets.

Results

Elevation comparison (vertical accuracy)

The RTK-GPS-generated point cloud included above-sea-level z values of the entire 27,307 location points; this was envisioned as a reference platform. When the model was visualized, it was apparent that the recorded point spacing was sufficient to build a high-precision surface representation, either in TIN or in GRID format. A TIN-type functional surface model was initially generated, and because the nature of the point clouds was based on irregular spacing, a rather precise topographic representation of the area in question was achieved. SRTMv3, DLR, GDEMv1, and GDEMv2 DEMs were downloaded, having been previously resampled to a finer GRID size of 23 × 23 m, and the ALOS_P dataset, a dual-polarization fine beam mode, was downloaded in a 12.5 × 12.5-m GRID size, and they were all envisioned as comparison platforms. Elevation comparison was carried out in the following stages. First, a 23 × 23-m raster DEM was produced from the point cloud. A GRID spacing of 23 × 23 m was selected because this is the default spacing for the majority of the downloaded DEMs for creating a comparable platform between the point-cloud-derived DEM (reference) and the others (comparisons). Small GRID size ALOS PALSAR data was preserved as is, with the intention of seeing how a finer GRID spacing would perform in defining the intended parameters. Point cloud locations were laid on each DEM, and new elevation values were extracted from each of the comparison datasets. Vertical accuracies were computed in terms of root-mean-square error (RMSE) (Table 1). Moreover, the correlation coefficient (r) was calculated to check the strength of the relationship between the reference and comparison datasets (Table 2 and Fig. 3). DLR yielded the strongest relationship with an r value of 0.98961.

All comparison datasets yielded satisfactory results, but the DLR, ALOS_P, and SRTMv3 rasters were similar and yielded better fits than those of GDEMv1 and GDEMv2.

A percent slope map was then produced from the reference dataset to visualize the distribution of elevation values across the slope categories. The slope was categorized into eight classes by slightly modifying the Food and Agriculture Organization's "Guidelines for Soil Description" as follows (FAO 2006): $\leq 1\%$ (*flat*), $1 < \% \leq 2$ (*nearly level*, *very gently sloping*), $2 < \% \leq 5$ (*gently sloping*), $5 < \% \leq 10$ (*sloping*), $10 < \% \leq 15$ (*strongly sloping*), $15 < \% \leq 30$ (*moderately steep*), $30 < \% \leq 60$ (*steep*), $60 < \%$ (*very steep*). When the slope map was intersected with the point cloud (reference) and the DEM-derived (comparison) z values, the distribution of the elevation values with respect to the slope classes was achieved for all datasets (Table 3).

Analysis of the variance and mean of the comparisons was performed for the elevation data at the 5% significance level. The general linear model procedure for a two-factor unbalanced analysis of variance was performed to analyze the main effects and their interactions on the means of elevation. The factors were slope category (< 1, 2, 5, 10, 15, 30, 60, and > 60%) and raster

Table 1 Root-mean-square error of comparison on a 23 × 23-m raster

Residual statistics					
Variable	*N*	Mean	Minimum	Maximum	RMSE
DLR	27,307	−33	−61	19	34
SRTMv3	27,307	−5	−37	26	9
GDEMv1	27,307	−5	−78	40	14
GDEMv2	27,307	−10	−73	33	15
ALOS_P	27,307	−36	−64	3	37

Table 2 Correlation coefficients. Reference vs. comparisons on a 23 × 23 m raster

Pearson correlation coefficients, $N = 27{,}307$					
Prob > |r| under H0: Rho = 0					
	DLR	SRTMV3	GDEMV1	GDEMV2	ALOS_P
ELEVATION	0.98961	0.98720	0.95943	0.97317	0.98866
	< 0.0001	< 0.0001	< 0.0001	< 0.0001	< 0.0001

type (RTK-GPS-generated elevation, DLR, SRTMv3, GDEMv1, GDEMv2, and ALOS_P rasters) (Table 4).

SRTMv3 yielded similar results to those of the measured values (reference) in all slope categories, whereas GDEMv1 yielded the same results, except for the slope category < 1, and GDEMv2 was matched with the elevation values in categories < 1 and 60. Both DLR and ALOS_P rasters overestimated the measured elevation values in all slope categories.

Finally, DEMs specifying smaller GRID sizes of 8 × 8 m were produced for the comparison datasets, and a second set of elevation values were generated. As opposed to registering a constant elevation value anywhere on a raster cell (ESRI 2018), TIN inherently provides different elevation values on an identical façade (Bitelli and Carla 1997). This convinced us to produce a finer GRID to check whether similarity to the measured values could be achieved. The new spacing was roughly one-ninth of the original GRID spacing of 23 × 23 m (Tables 5 and 6). DLR yielded the strongest relationship with an r value of 0.99058 (Table 7).

Although some improvement was achieved, as can be seen in Table 6, the level of improvement was inadequate, so no further testing using the finer GRID spacing was performed.

Slope acreage comparison

Slope, which can also be defined as the steepness of a line, is the ratio of change in elevation with respect to horizontal change. In a linear setting, a slope is a constant ratio of change. It has an uninterrupted changing value within a domain. Geographic information system analysis functions that can use spatial and nonspatial data are employed to calculate slope values representing the topography at any given location. A plane can be derived from the changing elevation points at the location of interest (Aronof 2005; Grohmann 2015). In an elevation modeling scheme, since the slope is a parameter shaped in accordance with the neighboring elevation values, in order to determine the level of resemblance of the comparison slope maps to that of the reference slope map, the original RTK-GPS-generated point cloud was intersected with both the reference and the comparison slope maps, and matching slope category pairs were sought to determine which comparison slope map resembled the reference one. The X-band DLR slope map showed a 49% similarity to the reference slope map (Table 8). Although there are other proven means of generating DEMs with a rather high precision and sensitivity, such as light detection and ranging, microwave, and unmanned aerial vehicles (Yang et al. 2014; Che et al. 2014; Bhardwaj et al. 2016), the accessibility, extent, and costs of these approaches continue to limit their widespread use. Slope is ideally calculated either in degrees or in percentages (elevation gain/loss between two locations in connection with the horizontal distance) and was selected as one of the measured and compared watershed parameters because it is an important factor affecting fire behavior, solar heating, infiltration, erosion, and water flow in watershed-related works (Sturm and Podobnikar 2017; Hilton et al. 2016; Sullivan et al. 2014; López-Moreno et al. 2013; Shin et al. 2013; Jiang et al. 2014). It should be well defined to understand the reasoning behind its failure before any type of corrective procedure is implemented (Duncan et al. 2014). Slope was categorized into the eight previously mentioned classes. Later, vectorized slope maps were generated from both the reference and the comparison rasters. Finally, the acreages corresponding to each plane in all classes were computed in hectares. The resulting polygons were clustered together, and the final acreages were tabulated (Table 9 and Fig. 4).

There was no clear advantage for any of the comparison datasets over the others, but the clustered total slope acreages of the reference dataset in the slope categories 5, 15, and 60 were approximately the same as those

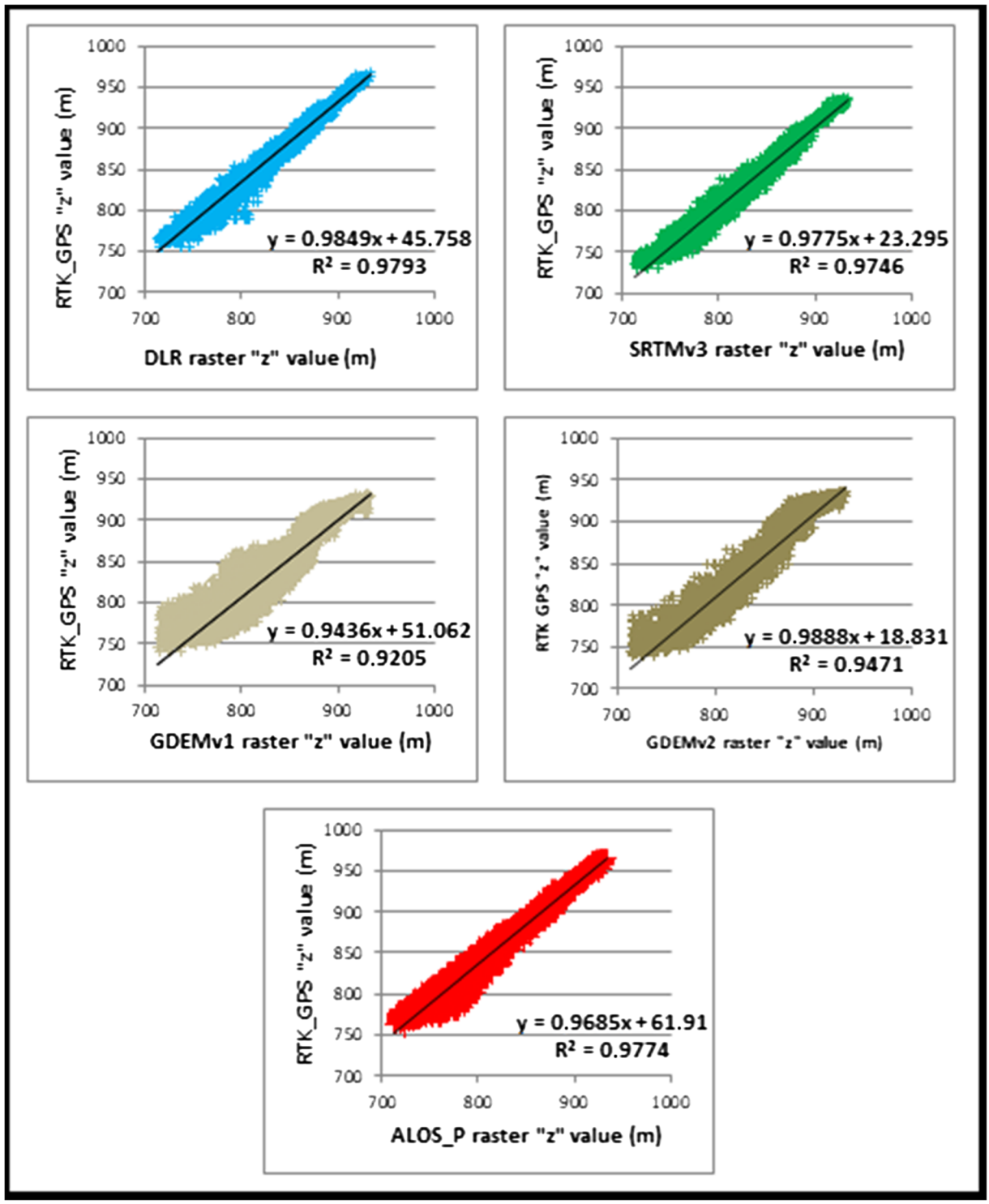

Fig. 3 Linear correlation between reference and comparison datasets on a 23 × 23-m raster

calculated using the ALOS_P dataset, whereas in the cases of the slope categories 10 and > 60 from DLR, the slope category < 1 from GDEMv1, the slope category 2 from SRTMv3, and the slope category 30 from GDEMv2 produced acreages close to those calculated over the reference dataset. The ALOS_P dataset was

Table 3 RTK-measured elevation values vs. 23 × 23-m DEM-extracted elevation values by slope code

RTK_Slp_ code	Elevation	DLR raster	SRTMv3 raster	GDEMv1 raster	GDEMv2 raster	Alsip raster
30	713,80	765	736	745	745	762
30	713,80	765	736	745	745	762
10	714,65	765	730	741	739	762
10	714,65	765	730	741	739	762
10	714,79	764	735	755	751	764

Table 4 Mean comparison of raster type within each slope category

Raster type	Slope category %							
	< 1	2	5	10	15	30	60	60 <
Elevation	873.792^{b*}	837.035^{c}	827.981^{c}	837.378^{c}	845.004^{c}	833.323^{c}	812.420^{b}	781.489^{c}
DLR_raster	906.415^{a}	872.228^{a}	863.360^{a}	872.285^{a}	879.447^{a}	867.514^{a}	845.221^{a}	812.405^{a}
SRTMv3_raster	877.566^{b*}	844.105^{bc}	835.305^{bc}	844.300^{bc}	851.136^{bc}	838.917^{bc}	816.460^{b}	784.464^{bc}
GDEMv1_raster	869.491^{c}	842.368^{bc}	835.412^{bc}	844.400^{bc}	850.132^{bc}	828.259^{bc}	815.158^{b}	790.698^{bc}
GDEMv2_raster	879.337^{b*}	848.084^{b}	840.084^{b}	848.115^{b}	855.475^{b}	843.252^{b}	820.886^{b}	792.322^{b}
Alos_P_raster	909.113^{a}	874.053^{a}	865.916^{a}	875.077^{a}	881.899^{a}	869.669^{a}	847.878^{a}	817.156^{a}

Raster types exhibited statistically different results within each slope category ($p < 0.005$)

$^{*, a, b}$ and ^{c} denote homogenous groups within slope categories

better at defining more slope categories simply because it acquired elevation data over a smaller GRID spacing than the rest.

Reservoir comparison

A common task when using a functional surface is to calculate the area and volume of a surface above or below a given reference plane. SRTM and other comparable open-access elevation models have been reported to create opportunities for dynamic surface elevation variations in mountain glaciers and coastal dune fields, among other features (Surazakov and Aizen 2006; Zhou et al. 2011; Grohmann and Sawakuchi 2013). For comparison, a scenario hypothesizing a reservoir, for which the 2D water surface area and 3D reservoir area and volume were sought below a water height of 800 m, was established for the study area in ArcScene 10. A plane intersecting the TIN-based elevation model of each dataset, that is, GPS data for reference and SRTM, GDEM, and PALSAR datasets for comparison, represented the water level at the specified height. In order to calculate the area and volume, the surface volume tool was used (Fig. 5). Elevation, as the input surface of the

Table 5 RTK-measured elevation values vs. 8 × 8-m DEM-extracted elevation values

Elevation	DLR raster	SRTMv3 raster	GDEMv1 raster	GDEMv2 raster	AlosP raster
713,80	764,07	734,92	744,28	742,69	761,41
713,80	766,07	736,67	746,12	744,13	762,07
714,65	763,02	730,79	741,53	739,00	762,39
714,65	763,02	731,98	742,90	740,29	762,39
714,79	763,02	733,68	751,45	745,73	765,25

Table 6 Root-mean-square error of comparison on an 8 × 8-m raster

Residual Statistics					
Variable	*N*	Mean	Minimum	Maximum	RMSE
DLR	27,307	− 33	− 60	17	34
SRTMV3	27,307	− 5	− 35	24	9
GDEMV1	27,307	− 5	− 78	39	14
GDEMV2	27,307	− 10	− 70	28	15
ALOS_P	27,307	− 36	− 62	3	37

Table 7 Correlation coefficients. Reference vs. comparisons on an 8 × 8-m raster

Pearson correlation coefficients, $N = 27{,}307$					
Prob > |r| under H0: Rho = 0					
	DLR	SRTMV3	GDEMV1	GDEMV2	ALOSPLR
Elevation	0.99058	0.98796	0.95994	0.97424	0.98880
	< 0.0001	< 0.0001	< 0.0001	< 0.0001	< 0.0001

calculations, was taken from the 3D elevation models. To ensure that the volume is less than the proposed water height, the option "below" was set on the reference plane, along with 800 m as the plane height. The resulting analysis generated both of the 2D and 3D areas, as well as the volume to be held in the reservoir. The 3D or surface area yielded larger figures because it was measured along the slope of the surface, and it considered the variation and height of the surface (Mukherjee et al. 2013). Unless the surface is flat, the surface area will always be greater than the ones calculated using the 2D area (Jenness 2004). To get an indication of the roughness or the slope of the surface, the 2D and surface areas can be compared. The larger the difference between the two values, the rougher or steeper the surface. Volume, by contrast, referred to the space in cubic map units between the surface and the reference plane at a particular height (Table 10). Calculations using SRTMv3 generated the closest values to those of the reference dataset in terms of volume, and GDEMv1 yielded results similar to those of the reference dataset in terms of acreage (Fig. 6).

Discussion

Turkey is projected to be a country that will be negatively influenced by the effects of global warming and climate change, which have been affecting the world since the last century. Thus, intensive work and projects are currently being carried out to counteract and minimize the consequences of desertification, land degradation, and drought, as well as their combined effects. Accordingly, the authorities are encouraging watershed management and rehabilitation projects that can convert unproductive forest covers into productive forests (Boydak and Caliskan 2015); diminish the levels of erosion and sedimentation (Mukundan et al. 2013); protect reservoirs, ponds, lakes, and rivers; and conserve arable lands (Ziadat and Taimeh 2013). Moreover, the dangers of torrents and landslides can be prevented, hence preserving life, livelihood, and commodity to ensure that future generations will prosper. The means to define watershed parameters are crucial in the effort to manage watersheds. Elevation, the intrinsic parameter of any digital surface representation, slope (acreage), and reservoir holding capacity, as extracted from various open-access DEMs, were compared to those of an RTK-GPS-generated point cloud and the resulting elevation model. SRTMv3 data yielded values rather close to those of the reference dataset, and the average absolute vertical accuracy was well within the published data specifications of ± 16 m, whereas the results obtained using X-band DLR data were overestimated by almost 200% compared to the global claim (Kolecka and Kozak 2014). The average

Table 8 Slope category comparison per elevation value. Zero denotes matching slope categories

Elevation	RTK	DLR	SRTM	Gdem1	Gdem2	Alos_P	RTK_DLR	RTK_Srtm	RTK_Gdem1	RTK_Gdem2	RTK_ALOS_P
713,80	30	60	60	30	60	15	− 30	− 30	0	− 30	15
713,80	30	60	60	30	60	15	− 30	− 30	0	− 30	15
714,65	10	30	15	15	10	30	− 20	− 5	− 5	0	− 20
714,65	10	30	15	15	10	30	− 20	− 5	− 5	0	− 20
714,79	10	30	30	60	60	30	− 20	− 20	− 50	− 50	− 20
714,79	10	30	30	60	30	60	− 20	− 20	− 50	− 20	− 50

Table 9 Clustered acreages based on slope categories of reference and comparison datasets

RTK_GPS (reference)		DLR (comparison 1)		SRTMv3 (comparison 2)		GDEMv1 (comparison 3)		GDEMv1 (comparison 4)		ALOS_P (comparison 5)	
RTK_R_A		DLR_R_A		SRTM_R_A		GDEMV1_R_A		GDEMV2_R_A		Alos_P_R_A	
G_C	A (ha)	G_C	A (ha)	G_C	A (ha)	G_C	A(ha)	G_C	A(ha)	G_C	A(ha)
1	0.29	1	0.16	1	0.11	1	0.38	1	0.16	1	0.05
2	0.41	2	0.59	2	0.55	2	0.84	2	0.93	2	0.24
5	1.78	5	2.59	5	2.19	5	4.51	5	4.03	5	1.55
10	6.79	10	8.32	10	11.86	10	19.49	10	11.99	10	9.65
15	14.53	15	17.25	15	18.28	15	27.86	15	17.92	15	15.19
30	56.84	30	66.25	30	72.54	30	68.83	30	62.32	30	67.39
60	61.48	60	57.31	60	53.36	60	39.12	60	58.35	60	60.10
61	21.99	61	11.63	61	5.22	61	3.08	61	8.42	61	9.96

R_A raster area, *G_C* gridcode, slope category

values obtained using both versions of GDEM were less than the values in the data validation reports (Aster Global DEM Validation 2009; Elkhrachy 2016). ALOS PALSAR's residual average was similar to that of the DLR dataset. Pearson's correlations between all comparison datasets and the reference dataset were strong, with slight variations in the results in the cases of DLR, ALOS_P, SRTMv3, GDEMv2, and GDEMv1; the corresponding correlation coefficients were 0.98961, 0.98866, 0.98720, 0.97317, and 0.95943, respectively, on the 23 × 23-m original rasters. Decreasing the cell size to 8 × 8 m did not change the sequence but rather strengthened the correlation slightly. Point distribution plots clarified the correlation results and explained the order better. The point distributions obtained using DLR, ALOS_P, and SRTMv3 were better dispersed compared to those of GDEMv1 and GDEMv2. However, the mean comparison performed at the 5% significance level showed that SRTMv3 extracted elevation values within each slope category that almost entirely matched the terrain-measured (reference) elevation values. The results obtained using GDEMv1 and GDEMv2 were close to the reference values. In all slope categories, calculations performed using the DLR and ALOS_P datasets yielded overestimated values. There was no clear winner in the elevation comparison, but it could be said that SRTMv3 with low residuals, which were compliant with the published verification residuals and better fit to the measured elevation values (reference), is the better choice over the other datasets. In terms of slope acreage comparison, the raster-to-vector conversion procedure was employed to generate slope maps, and computable polygons were generated. With the exception of ALOS_P, all the other raster datasets were processed over a 23 × 23-m GRID spacing. Owing to the differences in methodology, that is, using different wavelength radars or space-borne stereo image capturing (respective DEMs, comparison datasets), the slope acreages differed. In this terrain, the

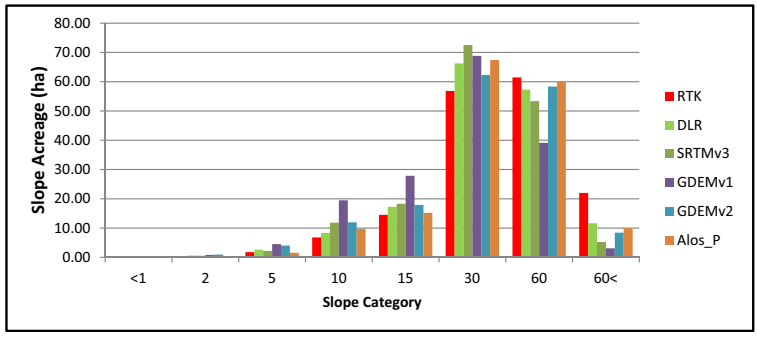

Fig. 4 Raster area acreage by slope category

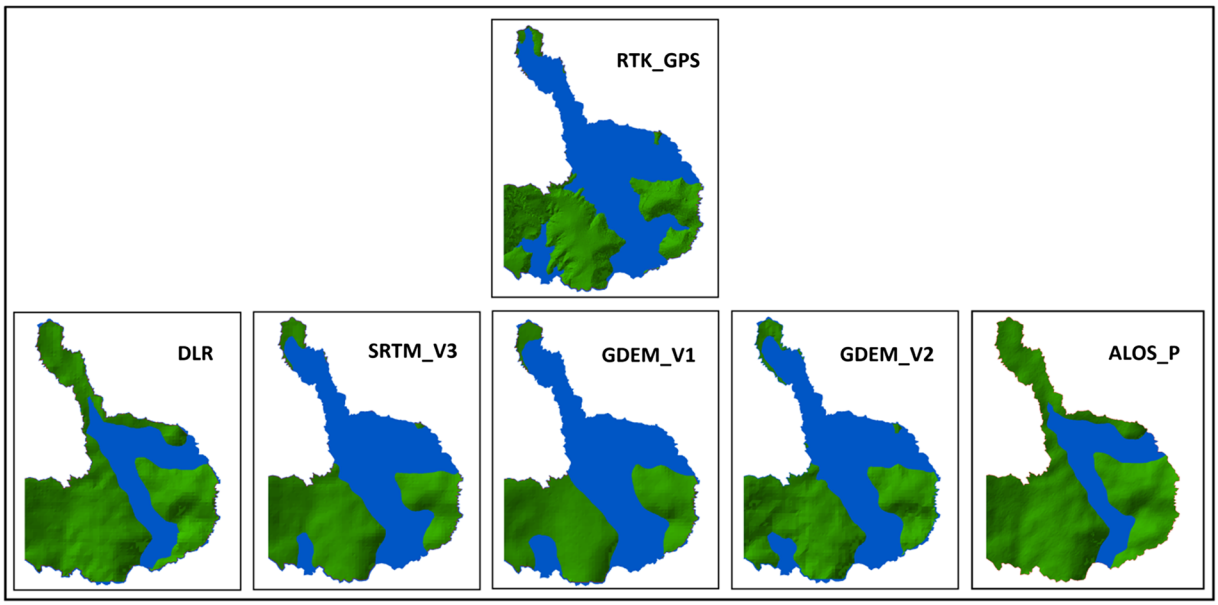

Fig. 5 Visualization of water at 800 m within the study area

bulk of all slope polygons was assigned to the slope categories 30 and 60. ALOS_P for slope category 60 and GDEMv2 for slope category 30 yielded acreages that were approximately the same as that of the reference dataset. Additionally, for slope categories 5 and 15, ALOS_P with a rather smaller GRID spacing yielded an acreage close to that of the reference dataset. The second-best result was obtained with the DLR dataset in slope categories 10 and > 60. The remaining categories were shared between SRTMv3 and GDEMv1 for the best comparison to the reference dataset. Using a smaller GRID spacing (12.5 m for ALOS PALSAR and 25 m for DLR_SRTM) is expected to produce similar results to those calculated from the terrestrial measurements, and they did indeed perform better. According to the results of a two-way slope comparison, the DLR slope map depicted 49% of the entire study area, which was the same as the reference data slope map, and SRTMv3, GDEMv1, GDEMv2, and ALOS_P depicted 35%, 17%, 9%, and 7%, respectively. In terms of reservoir capacity, we were concerned with a better representation of the area in question. One could expect that the smaller the GRID size, the better the surface definition. However, volume and area calculations made using SRTMv3 along with both GDEMv1 and GDEMv2 yielded results closer to those of the reference dataset. Both DLR and ALOS_P excessively underestimated in both calculations, justifying the extreme RMSE values in the residual statistics, meaning that both models varied significantly from the appropriate representation of the area in question.

Conclusion

Although many studies have been conducted to test the accuracy of open-access DEMs in various scenarios

Table 10 Reservoir area and capacity calculation

	RTK_GPS	DLR	SRTMv3	GDEMv1	GDEMv2	Alos_P
Plane_height	800	800	800	800	800	800
Reference	Below	Below	Below	Below	Below	Below
Z_factor	1	1	1	1	1	1
Area_2D (m^2)	552,312	214,453	508,661	538,189	467,707	197,720
Area_3D (m^2)	673,928	237,244	545,435	558,925	500,461	210,752
Volume (m^3)	16,220,383	3,502,125	13,197,742	11,915,414	10,706,389	2,546,897

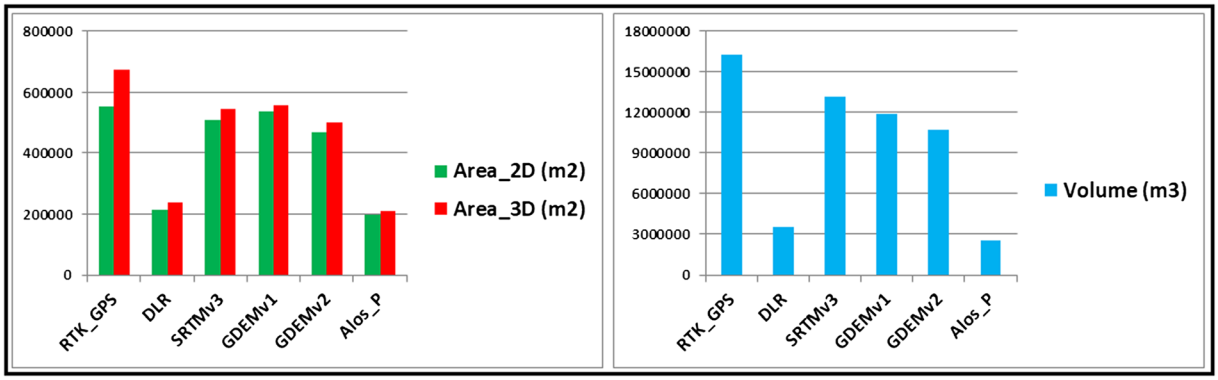

Fig. 6 Area and volume comparisons for all models

throughout the world, the varying topography in Turkey requires attention because every attempt to develop the country deals with a clear definition of the bare earth. Thus, providing examples to provide feedback for such an agenda is important. The vertical accuracy testing of DEMs was, therefore, not the main focus of this study, but finding a DEM that provides a good fit to the actual topography was deemed more important. Furthermore, a good fit would better depict the morphological features of the area in question. At this point, the original spacing of 30 m, which was used in four out of the five comparison datasets adopted in this study, was found to be a medium-level resolution that would obviously miss a considerable amount of fine detail. Additionally, the orientation of the radar beam would yield different elevation values even if the same GRID spacing was to be used because each pixel corner vertex would return a different timing, generating a different elevation value, even from the same topography. This is probably what was encountered in this study of medium-level DEMs. The original structuring of the resolution of the open-access DEMs was rather coarse for producing intricate work in treacherous topographies. Five open-access DEMs and DEM-extracted information were compared to an RTK-GPS-generated point cloud and the resulting elevation model for a few watershed parameters in a small watershed. The study was designed to determine the precision of the DEMs in a rather confined but diverse topography. SRTMv3 proved satisfactory in the residual, correlation, mean, and reservoir capacity comparisons. ALOS PALSAR and DLR_SRTM were able to define a greater number of slope categories than the others. Finally, DLR_SRTM and SRTMv3 matched more slope façades and scored higher than the other datasets. Aside from the ones tested in this study, other engineering-related parameters can be extracted from DEMs; however, there has not been one perfect global elevation model responding flawlessly to all sorts of planning and decision-making necessities. There are both strong and weak sides to all such models. In order to firmly validate the results, a larger area needs to be surveyed and the models need to be compared, but it is clear that SRTM data and its derivatives will still continue to provide valuable feedback for topographical surface definitions in the years to come.

References

Aguilar, F. J., Agüera, F., Aguilar, M. A., & Carvajal, F. (2005). Effects of terrain morphology, sampling density, and interpolation methods on grid DEM accuracy. *Photogrammetric Engineering and Remote Sensing, 71*(7), 805–816.

Anornu, G. K., & Kortatsi, B. K. (2012). Comparability studies of high and low resolution digital elevation models for watershed delineation in the tropics: Case of Densu River basin of Ghana. *International Journal of Cooperative Studies., 1*(1), 9–14.

Aronof, S. (2005). *Remote sensing for GIS managers. First.* Redlands: ESRI Press 487 p.

Asmamaw, D. K. (2015). A critical review of integrated river basin management in the upper Blue Nile river basin: The case of Ethiopia. *International Journal of River Basin Management, 13*(4), 429–442.

Aster Global DEM Validation (2009). Summary report. 28 p. Available online at https://lpdaac.usgs.gov/sites/default/files/public/aster/docs/ASTER_GDEM_Validation_Summary_Report.pdf, last accessed 28 July 2017.

Benda, L., Miller, D., Barquin, J., McCleary, R., Cai, T. J., & Ji, Y. (2016). Building virtual watersheds: A global opportunity to strengthen resource management and conservation. *Environmental Management, 57*(3), 722–739.

Berthier, E., Schiefer, E., Clarke, G., Menounos, B., & Rémy, F. (2010). Contribution of Alaskan glaciers to sea-level rise derived from satellite imagery. *Nature Geoscience, 3*, 92–95.

Bhardwaj, A., Sam, L., Akanksha, F., Martín-Torres, J., & Kumar, R. (2016). UAVs as remote sensing platform in glaciology: Present applications and future prospects. *Remote Sensing of Environment, 175*, 196–204.

Bitelli, A. C. G., & Carla, R. (1997). Comparison of techniques for generating digital terrain models from contour lines. *International Journal of Geographical Information Science, 11*(5), 451–473.

Bolt, B. A., Horn, W. L., MacDonald, G. A. & Scott, R. F. (2013). Geological hazards: earthquakes - tsunamis - volcanoes - avalanches - landslides - floods. Revised, Second edition. Springer Science & Business Media. 332 p.

Boydak, M. & Caliskan, S. (2015). Afforestation in arid and semi-arid regions. 68 p. Available online at: http://www.cem.gov.tr/erozyon/Files/yayinlarimiz/AFFORESTATIONINARIDANDSEMIARIDREGIONS.pdf, last accessed 25 July 2018.

Ceylan, A., Alan, I. & Ugurlu, A. (2007). Causes and effects of flood hazards in Turkey. *The proceedings of International Congress River Basin Management*. Antalya, Turkey: 415–423.

Che, T., Li, X., Jin, R., & Huang, C. (2014). Assimilating passive microwave remote sensing data into a land surface model to improve the estimation of snow depth. *Remote Sensing of Environment, 143*, 54–63.

Deniz, R., Celik, R. N., Kutoglu, H., Ozludemir, M. T., Demir, C. & Kinik, I. (2008). Buyuk Olcekli Harita ve Harita Bilgileri Uretim Yonetmeligi. 86 p. Available online at: http://www.hkmo.org.tr/resimler/ekler/7VST_ff3e350028d0cfc_ek.pdf, last accessed 16 July 2018.

Duncan, J. M., Wright, S. G., & Brandon, T. L. (2014). *Soil strength and slope stability* (2nd ed.). John Wiley and Sons, Inc.: Hoboken 317 p.

Elkhrachy, I. (2016). Vertical accuracy assessment for SRTM and ASTER Digital Elevation Models: A case study of Najran city, Saudi Arabia. *Ain Shams Engineering Journal, 2*, 1–11.

EM-DAT (2009). Center for Research on the epidemiology of disasters. Available online at: http://www.emdat.be/database, last accessed 16 Mar 2017.

ESRI (2018). What is raster data?—Help | ArcGIS for desktop. Available online at: http://desktop.arcgis.com/en/arcmap/10.3/manage-data/raster-and-images/what-is-raster-data.htm, last accessed 16 July 2018.

FAO (2006). Guidelines for soil description. Fourth. Food and Agriculture Organization of the United Nations, Rome. 109 p. Available online at: http://www.fao.org/3/a-a0541e.pdf, last accessed 16 July 2018.

Gao, J. (1997). Resolution and accuracy of terrain representation by grid dems at a micro-scale. *International Journal of Geographical Information Science, 11*(2), 199–212.

Golding, B., Roberts, N., Leoncini, G., Mylne, K., & Swinbank, R. (2016). MOGREPS-UK convection-permitting ensemble products for surface water flood forecasting: Rationale and first results. *Journal of Hydrometeorology, 17*, 1383–1406.

Goulden, T., Hopkinson, C., Jamieson, R., & Sterling, S. (2016). Sensitivity of DEM, slope, aspect and watershed attributes to LiDAR measurement uncertainty. *Remote Sensing of Environment, 179*, 23–35.

Grohmann, C. H. (2015). Effects of spatial resolution on slope and aspect derivation for regional-scale analysis. *Computational Geosciences, 77*, 111–117.

Grohmann, C. H., & Sawakuchi, A. O. (2013). Influence of cell size on volume calculation using digital terrain models: A case of coastal dune fields. *Geomorphology, 180-181*, 130–136.

Grussenmeyer, P., Landes, T., Voegtle, T., & Ringle, K. (2008). Comparison methods of terrestrial laser scanning, photogrammetry and tachometry data for recording of cultural heritage buildings. *The International Archives of the Photogrammetry, Remote Sensing and Spatial Information Sciences, XXXVI*, 213–218.

Hilton, J. E., Miller, C., Sharples, J. J., & Sullivan, A. L. (2016). Curvature effects in the dynamic propagation of wildfires. *International Journal of Wildland Fire, 25*(12), 1238–1251.

Jenness, J. S. (2004). Calculating landscape surface area from digital elevation models. *Wildlife Society Bulletin, 32*(3), 829–839.

Jiang, S.-H., Li, D.-Q., Zhang, L.-M., & Zhou, C.-B. (2014). Slope reliability analysis considering spatially variable shear strength parameters using a non-intrusive stochastic finite element method. *Engineering Geology, 168*(86), 120–128.

Józsa, E., Fábián, S. Á., & Kovács, M. (2014). An evaluation of EU-DEM in comparison with ASTER GDEM, SRTM and contour-based DEMs over the Eastern Mecsek Mountains. *Hungerian Geographic Bulletin., 63*(4), 401–423.

Kang, M., Wang, M., & Du, Q. (2015). A method of DTM construction based on quadrangular irregular networks and related error analysis. *PLoS One, 10*(5), 1–17.

Kolecka, N., & Kozak, J. (2014). Assessment of the accuracy of SRTM C- and X-Band High Mountain Elevation Data: A case study of the Polish Tatra Mountains. *Pure and Applied Geophysics, 171*(6), 897–912.

Kweon, I. S., & Kanade, T. (1994). Extracting topographic terrain features from elevation maps. *Cvgip:Image Underst., 59*(2), 171–182.

López-Moreno, J. I., Revuelto, J., Gilaberte, M., Morán-Tejeda, E., Pons, M., Jover, E., Esteban, P., García, C., & Pomeroy, J. W. (2013). The effect of slope aspect on the response of snowpack to climate warming in the Pyrenees. *Theoretical and Applied Climatology, 117*(1), 207–219.

Mahmood, S., Khan, A. u. H., & Ullah, S. (2016). Assessment of 2010 flash flood causes and associated damages in Dir Valley, Khyber Pakhtunkhwa Pakistan. *International Journal of Disaster Risk Reduction, 16*, 215–223.

Mei, Y., Chang, C., Dong, Z., & Wei, L. (2016). Stream, Lake, and reservoir management. *Water Environment Research, 87*(10), 1515–1550.

Mispan, M. R., Zamir, M., Rasid, A., Faiza, N., Rahman, A., Haron, S. H., & Ahmad, N. (2015). Assessment of ASTER and SRTM derived digital elevation model for highland areas of peninsular Malaysia region. *Concepts Journal of Applied Research., 02*(09), 316–320.

Mukherjee, S., Joshi, P. K., Mukherjee, S., Ghosh, A., Garg, R. D., & Mukhopadhyay, A. (2013). Evaluation of vertical accuracy of open source digital elevation model (DEM). *International Journal of Applied Earth Observation and Geoinformation., 21*, 205–217.

Mukundan, R., Pradhanang, S. M., Schneiderman, E. M., Pierson, D. C., Anandhi, A., Zion, M. S., Matonse, A. H., Lounsbury,

D. G., & Steenhuis, T. S. (2013). Suspended sediment source areas and future climate impact on soil erosion and sediment yield in a New York City water supply watershed, USA. *Geomorphology., 183*, 110–119.

Munir, B. A., & Iqbal, J. (2016). Flash flood water management practices in Dera Ghazi Khan City (Pakistan): A remote sensing and GIS prospective. *Natural Hazards, 81*(2), 1303–1321.

Nichol, J. E., Shaker, A., & Wong, M. S. (2006). Application of high-resolution stereo satellite images to detailed landslide hazard assessment. *Geomorphology, 76*(1–2), 68–75.

Patel, A., Katiyar, S. K., & Prasad, V. (2016). Performances evaluation of different open source DEM using differential global positioning system (DGPS). *The Egyptian Journal of Remote Sensing and Space Sciences, 19*(1), 7–16.

Pradhan, B. & Abdulwahid, W. M. (2017). Landslide risk assessment using multi-hazard scenario produced by logistic regression and LiDAR-based DEM in *Laser Scanning Applications in Landslide Assessment*: 253–275.

Risbøl, O., Briese, C., Doneus, M., & Nesbakken, A. (2015). Monitoring cultural heritage by comparing DEMs derived from historical aerial photographs and airborne laser scanning. *Journal of Cultural Heritage, 16*(2), 202–209.

Rufino, G., Moccia, A., & Esposito, S. (1998). DEM generation by means of ERS tandem data. *IEEE Transactions on Geoscience and Remote Sensing., 36*(6), 1905–1912.

Shin, H., Kim, Y. T., & Park, D. K. (2013). Development of rainfall hazard envelope for unsaturated infinite slope. *KSCE Journal of Civil Engineering, 17*(2), 351–356.

Sturm, T., & Podobnikar, T. (2017). A probability model for long term forest fire occurrence in the karst forest management area of Slovenia. *International Journal of Wildland Fire., 26*, 399–412.

Sullivan, A. L., Sharples, J. J., Matthews, S., & Plucinski, M. P. (2014). A downslope fire spread correction factor based on landscape-scale fire behaviour. *Environmental Modelling and Software., 62*, 153–163.

Surazakov, A. B., & Aizen, V. B. (2006). Estimating volume change of mountain glaciers using SRTM and map-based topographic data. *IEEE Transactions on Geoscience and Remote Sensing, 44*(10), 2991–2995.

Tayanc, M., Im, U., Dogruel, M., & Karaca, M. (2009). Climate change in Turkey for the last half century. *Climatic Change, 94*(3–4), 483–502.

Turker, A. & Acikgoz, T. (2006). Orman Isletmelerinin Etkinliklerine Iliskin Finansal Cozumlemeler in the *Proceedings of* "*Ormancilikta Sosyo Ekonomik Sorunlar Kongresi*" *_2006. Cankiri*: 163–173. Available online at: http://www.foresteconomics.org/congress/proceedings_2006.pdf, last accessed 25 July 2018.

Turner, K. G., Anderson, S., Gonzalez, M., Costanza, R., Courville, S., Dominati, E. & Ogilvy, S. (2014). Toward an integrated ecology and economics of land degradation and restoration: Methods, data, and models. *Report to the ELD Project Data and Methodology Working Group*: 1–60.

Uysal, M., Toprak, A. S., & Polat, N. (2015). DEM generation with UAV photogrammetry and accuracy analysis in Sahitler hill. *Measurement, 73*, 539–543.

Yang, R., Chang, Z. & Xue, T. (2011). 3D terrain visualization for Mountain Taishan. *ICSDM 2011 - Proc. 2011 IEEE Int. Conf. Spat. Data Min. Geogr. Knowl. Serv*:285–290. Available online at: https://ieeexplore.ieee.org/stamp/stamp.jsp?tp=&arnumber=5969048, last accessed 25 July 2018.

Yang, P., Ames, D. P., Fonseca, A., Anderson, D., Shrestha, R., Glenn, N. F., & Cao, Y. (2014). What is the effect of LiDAR-derived DEM resolution on large-scale watershed model results? *Environmental Modelling and Software, 58*, 48–57.

Zhou, J., Li, Z., & Xing, Q. (2011). Monitoring thickness changes of mountain glacier by differential interferometry of ALOS PALSAR data. IEEE International Geoscience and Remote Sensing Symposium, 24-29 July 2011, Vancouver, BC, CANADA, 3649–3652.

Ziadat, F. M., & Taimeh, A. Y. (2013). Effect of rainfall intensity, slope, land use and antecedent soil moisture on soil erosion in an arid environment. *Land Degradation and Development, 24*(6), 582–590.